PROCEEDINGS A

royalsocietypublishing.org/journal/rspa

Research

Cite this article: Choi GPT, Chen S, Mahadevan L. 2020 Control of connectivity and rigidity in prismatic assemblies. *Proc. R. Soc. A* **476**: 20200485.
https://doi.org/10.1098/rspa.2020.0485

Received: 22 June 2020
Accepted: 11 November 2020

Subject Areas:
materials science, applied mathematics, statistical physics

Keywords:
prismatic assemblies, rigidity, connectivity, percolation

Author for correspondence:
L. Mahadevan
e-mail: lmahadev@g.harvard.edu

THE ROYAL SOCIETY
PUBLISHING

Control of connectivity and rigidity in prismatic assemblies

Gary P. T. Choi[1,2], Siheng Chen[1] and L. Mahadevan[1,3,4]

[1]John A. Paulson School of Engineering and Applied Sciences, Harvard University, Cambridge, MA, USA
[2]Department of Mathematics, Massachusetts Institute of Technology, Cambridge, MA, USA
[3]Department of Physics, and [4]Department of Organismic and Evolutionary Biology, Harvard University, Cambridge, MA, USA

GPTC, 0000-0001-5407-9111; SC, 0000-0002-5494-0853; LM, 0000-0002-5114-0519

How can we manipulate the topological connectivity of a three-dimensional prismatic assembly to control the number of internal degrees of freedom and the number of connected components in it? To answer this question in a deterministic setting, we use ideas from elementary number theory to provide a hierarchical deterministic protocol for the control of rigidity and connectivity. We then show that it is possible to also use a stochastic protocol to achieve the same results via a percolation transition. Together, these approaches provide scale-independent algorithms for the cutting or gluing of three-dimensional prismatic assemblies to control their overall connectivity and rigidity.

1. Introduction

Given a three-dimensional solid, how can we introduce cuts in it that convert it to a prismatic assembly that is either partially or fully connected, and can be either partially or completely rigid? Said differently, how does the topology of the underlying network of connectivity in such an assembly control the degrees of freedom (DoF) and the number of connected components (NCC), i.e. the number of distinct clusters? And how can we use either deterministic or stochastic approaches to control both these properties? Here, we explore and answer these questions using a combination of analysis and computation. In addition to being of intrinsic interest, the questions are of technological relevance for understanding the assembly of polyhedral building blocks into ordered structures in atomic systems [1] as well as the design of molecular materials [2] and nanocrystals [3].

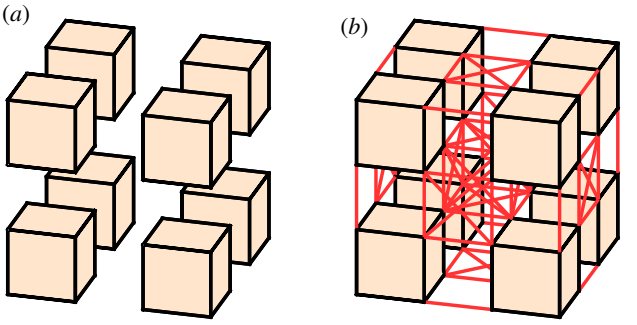

Figure 1. Topological control of prismatic assemblies is analogous to controlling a linkage. (*a*) An example of how a solid can be decomposed into an $L \times M \times N$ three-dimensional prismatic assembly (here $L = M = N = 2$). (*b*) All possible links for connecting neighbouring cubes in a $2 \times 2 \times 2$ prismatic assembly. A subset of these can be used to control the number of connected components, while another can be used to control the number of internal degrees of freedom in the assembly. Note that the wide separations between the cubes employed in this figure and all following figures in this paper are just for illustrative purposes. All links considered are infinitesimal and only used for representing the connectivity of the cubes. (Online version in colour.)

In the context of the problem raised above, the transition from a floppy phase to a rigid phase has been extensively studied within the framework of amorphous jamming induced by adding or removing linkages (constraints) in the network model [4–10]. More recently, it has also been shown that it is possible to tune the mechanical properties of the network near isostaticity (close to jamming) [11–15] by pruning links according to different algorithms. However, most of these studies focus on the problem of controlling the mechanical properties of a network by abstracting the nodes as point masses.

Here, we deviate from this perspective in a fundamental way. By considering structural assemblies with building blocks made of three-dimensional objects with shapes, we allow for the separation of the total DoF from internal DoF (defined as the DoF associated with the relative rotational motion among the assemblies rather than the rigid body motion). By randomly adding or removing links and thus changing the linkage pattern, we find non-monotonic changes in the internal DoF, as well as the existence of percolation transitions associated with the onset of connectivity and rigidity. The use of prismatic assemblies with high translational symmetry enables us to control the rigidity and connectivity in a deterministic way with minimal redundancy. Inspired by ideas from elementary number theory, we design algorithms to control the rigidity and connectivity of prismatic structures by designing minimal-redundancy link patterns in a hierarchical manner. (Minimal-redundancy means that no links can be removed while keeping the overall rigidity properties.) This efficient design might shed light on the subject of structural assemblies, with connection to the classical rigidity theory [16] and self-assembly [17–19].

To simplify our discussion, we start with a rectangular solid D in $\mathbb{R}^3$ with parallel cuts introduced along equally spaced grid lines in the x-, y- and z-directions. Assuming that the length, width and height of D are all integer multiples of a positive number l, the cuts decompose D into $L \times M \times N$ identical solid cubes with side length l (figure 1*a*). Then, we consider placing a number of infinitesimal links either deterministically or stochastically to connect some of the cubes with their neighbours (figure 1*b*), thereby forming a three-dimensional solid assembly. Here, the infinitesimal links are considered to be of zero length. Every link added between two vertices of two cubes indicates that the two vertices are connected and occupy exactly the same point. We remark that in practice, the infinitesimal links considered in this work can be easily realized by physical hinges, ball joints, short ligaments, or other ways of connecting two objects, but do not change our qualitative results. The infinitesimal links control the topology of the assembly and hence affect its rigidity and connectivity in terms of DoF and NCC. We can

transform the cutting problem into a linkage problem that is similar in spirit to the set-up in the planar analogue: a kirigami structure [20].

2. Deterministic control of rectangular prismatic assemblies

We first explore the deterministic control of prismatic assemblies, and establish algorithmic protocols for determining the minimum number of links that can (i) rigidify a prismatic assembly so that it has no internal modes of motion (i.e. control the DoF) or (ii) connect a prismatic assembly (i.e. control the NCC).

(a) Minimum rigidifying link patterns

Since each cube has three translational DoF and three rotational DoF, the maximum total DoF of any $L \times M \times N$ prismatic assembly is $d = 6LMN$. If all links are added, the entire prismatic assembly is rigid and hence the minimum DoF is $d = 6$. This suggests that as links are gradually added to the system, the total DoF decreases and eventually the entire system becomes rigid. Therefore, it is natural to consider the minimum number of links needed to make the system rigid. This requires analysing the effect of each link on the DoF of the system. As the links are vertex-based, it is more convenient to assess the total DoF by considering each cube as eight vertices, with constraints given by the geometry of the cubes and the infinitesimal links.

By Dehn's rigidity theorem [16], any closed convex polyhedron with infinitesimally rigid faces is infinitesimally rigid. Therefore, for each solid cube with side length l, there are exactly 12 *edge length constraints* in the form of

$$g_{\text{edge}}(\boldsymbol{v}_i, \boldsymbol{v}_j) = \|\boldsymbol{v}_i - \boldsymbol{v}_j\|^2 - l^2 = 0, \tag{2.1}$$

where $\boldsymbol{v}_i$ and $\boldsymbol{v}_j$ are two adjacent vertices in a cube, and six *diagonal length constraints* for all faces of the cube

$$g_{\text{diagonal}}(\boldsymbol{v}_i, \boldsymbol{v}_j) = \|\boldsymbol{v}_i - \boldsymbol{v}_j\|^2 - 2l^2 = 0, \tag{2.2}$$

where $\boldsymbol{v}_i$ and $\boldsymbol{v}_j$ are a pair of opposite vertices in a face. As an example, a rigid cube has 8 nodes (24 DoF), 12 edges (12 edge length constraints) and 6 faces (6 diagonal length constraints). The remaining number of DoF is $24 - 12 - 6 = 6$, which corresponds to the three translational and the three rotational DoF.

Note that there are in total $24LMN$ variables for the coordinates of all vertices, and we denote them as $x_1, x_2, x_3, \ldots, x_{24LMN}$, with $(x_{3i-2}, x_{3i-1}, x_{3i})$ being the coordinates of the vertex $\boldsymbol{v}_i$, $i = 1, 2, \ldots, 8LMN$. Now, adding a link between two vertices $\boldsymbol{v}_i = (x_{3i-2}, x_{3i-1}, x_{3i})$ and $\boldsymbol{v}_j = (x_{3j-2}, x_{3j-1}, x_{3j})$ in two neighbouring cubes imposes three *link constraints*

$$\left.\begin{aligned} g_{\text{link}_x}(\boldsymbol{v}_i, \boldsymbol{v}_j) &= x_{3i-2} - x_{3j-2} = 0, \\ g_{\text{link}_y}(\boldsymbol{v}_i, \boldsymbol{v}_j) &= x_{3i-1} - x_{3j-1} = 0 \\ \text{and} \qquad g_{\text{link}_z}(\boldsymbol{v}_i, \boldsymbol{v}_j) &= x_{3i} - x_{3j} = 0. \end{aligned}\right\} \tag{2.3}$$

We note that the decrease in DoF by adding a link can either be 0, 1, 2 or 3. If n links are added to the $L \times M \times N$ prismatic assembly, there will be in total $18LMN + 3n$ constraints ($18LMN$ length constraints and $3n$ link constraints). To determine the infinitesimal DoF d of the prismatic assembly, it is necessary to count the number of independent constraints. This can be done by the rigidity matrix rank computation [21,22]

$$d = 24LMN - \text{rank}(A), \tag{2.4}$$

where A is a rigidity matrix with the dimension $(18LMN + 3n) \times 24LMN$, and $A_{ij} = \partial g_i / \partial x_j$ for all i, j storing the partial derivatives of all above-mentioned constraints. We remark that this approach of calculating DoF is analogous to the application of the Calladine index theorem for connecting the number of zero modes to the rank of the compatibility matrix in an elastic network [23]. In

particular, the states of self-stress therein are equivalent to the zero energy states in our problem, which form the null space of the rigidity matrix A.

To determine the optimal lower bound of links needed to rigidify the assembly, we denote $\delta_{3D}(L,M,N)$ as the minimum number of links for rigidifying an $L\times M\times N$ prismatic assembly. Then we have

$$6LMN-3\delta_{3D}(L,M,N)\le 6. \tag{2.5}$$

This implies that

$$\delta_{3D}(L,M,N)\ge \frac{6LMN-6}{3}=2LMN-2. \tag{2.6}$$

Therefore, link patterns with less than $2LMN-2$ links can never rigidify an $L\times M\times N$ prismatic assembly. It is natural to ask whether the above lower bound is optimal (tight) for any combination of positive integers L,M,N. Denote a link pattern with exactly $2LMN-2$ links that can rigidify an $L\times M\times N$ prismatic assembly as a *minimum rigidifying link pattern* (MRP) for $L\times M\times N$. Below, we devise a *hierarchical construction* method for creating MRPs for infinitely many L,M,N.

To illustrate the idea of the hierarchical construction, here we first consider the case where $L=M=N$ and simplify the notation $\delta_{3D}(L,M,N)$ as $\delta_{3D}(L)$. Suppose MRPs exist for $l_1\times l_1\times l_1$ and $l_2\times l_2\times l_2$, i.e. $\delta_{3D}(l_1)=2l_1^3-2$ and $\delta_{3D}(l_2)=2l_2^3-2$. If we treat an $l_1l_2\times l_1l_2\times l_1l_2$ prismatic assembly as $l_2\times l_2\times l_2$ large blocks with size $l_1\times l_1\times l_1$, we can rigidify each large block using an MRP for $l_1\times l_1\times l_1$ (which consists of exactly $\delta_{3D}(l_1)$ links) and then rigidify the entire structure using an MRP for $l_2\times l_2\times l_2$ (which consists of exactly $\delta_{3D}(l_2)$ links). Thus, the whole $l_1l_2\times l_1l_2\times l_1l_2$ prismatic assembly is rigidified, with the total number of links

$$l_2^3\delta_{3D}(l_1)+\delta_{3D}(l_2)=l_2^3(2l_1^3-2)+(2l_2^3-2)=2(l_1l_2)^3-2. \tag{2.7}$$

This suggests that the link pattern constructed this way is an MRP for $l_1l_2\times l_1l_2\times l_1l_2$, i.e. $\delta_{3D}(l_1l_2)=2(l_1l_2)^3-2$. Using this idea of constructing larger MRPs via a hierarchical combination of smaller MRPs, we can prove that MRPs exist for all $L\times L\times L$ prismatic assembly with $L\ge 2$:

Theorem 2.1. *For all positive integer $L\ge 2$, we have*

$$\delta_{3D}(L)=2L^3-2. \tag{2.8}$$

Proof. We first explicitly construct MRPs for $L\times M\times N=2\times 2\times 2$, $3\times 3\times 3$, $2\times 2\times 3$, $2\times 3\times 3$, each with exactly $2LMN-2$ links (figure 2*a–d*), with the DoF of these assemblies verified computationally using equation (2.4). The existence of such patterns shows that the statement is true for $L=2,3$.

For $L\ge 4$, we prove the statement by induction. Suppose the statement is true for all positive integers less than L. Note that for $L\ge 4$, there always exists non-negative integers a,b with $a+b\ge 2$ such that $L=2a+3b$: If $L\equiv 0\ (\mathrm{mod}\ 3)$, we have $L=2\times 0+3\times\frac{L}{3}$. If $L\equiv 1\ (\mathrm{mod}\ 3)$, we have $L=2\times 2+3\times(L-4)/3$. If $L\equiv 2\ (\mathrm{mod}\ 3)$, we have $L=2\times 1+3\times(L-2)/3$.

Now, we decompose the $L\times L\times L$ prismatic assembly into $(a+b)\times(a+b)\times(a+b)$ blocks with size $2\times 2\times 2$, $2\times 2\times 3$, $2\times 3\times 3$ and $3\times 3\times 3$ (figure 2*e*). Since $2\le a+b<L$, by the induction hypothesis, the number of links connecting these blocks is

$$\delta_{3D}(a+b)=2(a+b)^3-2. \tag{2.9}$$

Therefore, if we first rigidify each block by the corresponding MRP in figure 2*a–d* and then rigidify the entire structure by an MRP for $(a+b)\times(a+b)\times(a+b)$, we obtain a rigidifying link pattern for the $L\times L\times L$ prismatic assembly, with the total number of links

$$\begin{aligned}&a^3\delta_{3D}(2)+b^3\delta_{3D}(3)+3a^2b\delta_{3D}(2,2,3)+3ab^2\delta_{3D}(2,3,3)+\delta_{3D}(a+b)\\&=14a^3+52b^3+66a^2b+102ab^2+2(a+b)^3-2\\&=16a^3+54b^3+72a^2b+108ab^2-2\end{aligned}$$

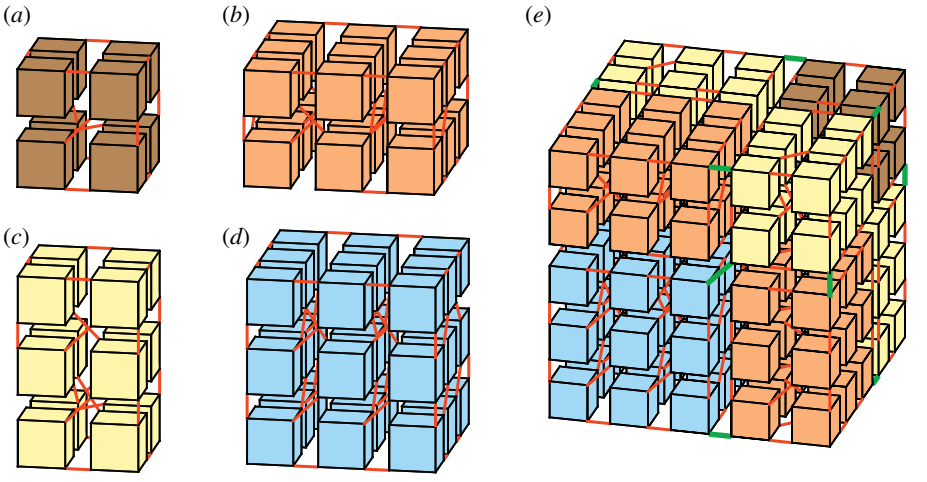

Figure 2. Minimum rigidifying link patterns (MRPs) and the hierarchical construction protocol for prismatic assemblies. (*a*) An MRP with exactly $2 \times 2^3 - 2 = 14$ links for a $2 \times 2 \times 2$ prismatic assembly. (*b*) An MRP with exactly $2 \times 2 \times 3 \times 3 - 2 = 34$ links for a $2 \times 3 \times 3$ prismatic assembly. (*c*) An MRP with exactly $2 \times 2 \times 2 \times 3 - 2 = 22$ links for a $2 \times 2 \times 3$ prismatic assembly. (*d*) An MRP with exactly $2 \times 3 \times 3 \times 3 - 2 = 52$ links for a $3 \times 3 \times 3$ prismatic assembly. For all four examples, we have checked that DoF $= 6$ using the rigidity matrix rank computation. (*e*) To construct an MRP for a $5 \times 5 \times 5$ prismatic assembly, we treat the $5 \times 5 \times 5$ cubes as eight large rectangular blocks with size $2 \times 2 \times 2$, $2 \times 2 \times 3$, $2 \times 3 \times 3$ and $3 \times 3 \times 3$ (each type is shown in a different colour). We rigidify each block using an MRP in (*a–d*) (the red links), and then connect and rigidify the entire structure using an MRP for $2 \times 2 \times 2$ (the green links), thereby obtaining an MRP for $5 \times 5 \times 5$ (see text for details). (Online version in colour.)

$$= 2(2a + 3b)^3 - 2$$
$$= 2L^3 - 2. \tag{2.10}$$

This implies that $\delta_{3D}(L) = 2L^3 - 2$. By induction, the statement is true for all $L \geq 2$. ■

Here, we remark that MRPs for a specific system size are not unique. One reason is that it is possible to rotate the MRPs shown in figure 2 during the hierarchical construction, which can lead to distinct MRPs. There may also be MRPs that are not covered by the proof of theorem 2.1 (i.e. not in the form of MRPs of MRPs of the intermediate blocks). Nevertheless, the hierarchical construction provides a systematic approach for creating MRPs for any system size L.

Furthermore, we can explicitly construct MRPs for infinitely many L, M, N:

Theorem 2.2. *For infinitely many positive integers L, M, N that are not all identical, we have*

$$\delta_{3D}(L, M, N) = 2LMN - 2. \tag{2.11}$$

Proof. Take any set of non-negative integers a_l, b_l, a_m, b_m, a_n, b_n such that $a_l + b_l = a_m + b_m = a_n + b_n \geq 2$ and

$$\left.\begin{aligned} L &= 2a_l + 3b_l, \\ M &= 2a_m + 3b_m \\ \text{and} \quad N &= 2a_n + 3b_n \end{aligned}\right\} \tag{2.12}$$

are not all identical (e.g. $(a_l, b_l, a_m, b_m, a_n, b_n) = (1, 6, 2, 5, 3, 4)$, with $(L, M, N) = (20, 19, 18)$). Then, we can decompose an $L \times M \times N$ prismatic assembly into $(a_l + b_l) \times (a_m + b_m) \times (a_n + b_n)$ small blocks of size $2 \times 2 \times 2$, $2 \times 2 \times 3$, $2 \times 3 \times 3$ and $3 \times 3 \times 3$. Since $a_l + b_l = a_m + b_m = a_n + b_n$, following the proof of theorem 2.1, we rigidify each small block and then the entire structure

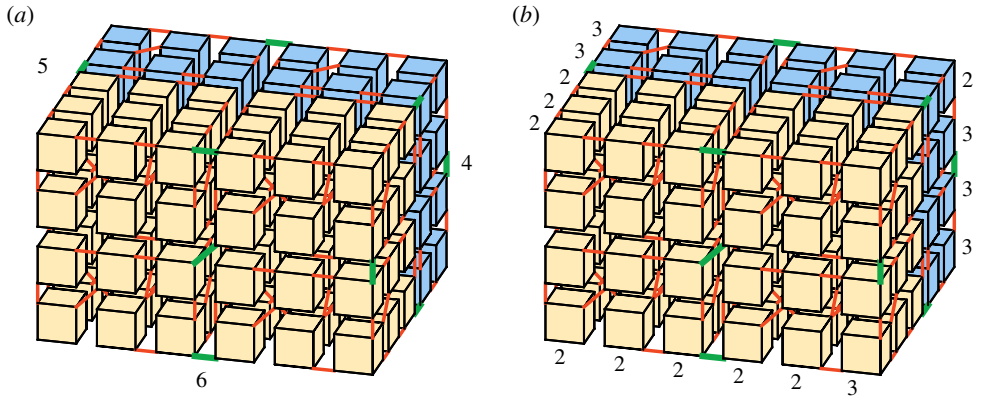

Figure 3. More examples of minimum rigidifying link patterns (MRPs) for rectangular prismatic assemblies. (*a*) An MRP for a $4 \times 5 \times 6$ rectangular prismatic assembly, consisting of four MRPs for $2 \times 3 \times 3$ (the blue cubes and the associated red links), four MRPs for $2 \times 2 \times 3$ (the yellow cubes and the associated red links) and an MRP for $2 \times 2 \times 2$ connecting the eight large blocks (the green links). (*b*) An MRP for an $11 \times 12 \times 13$ rectangular prismatic assembly can be constructed hierarchically using the MRP for $4 \times 5 \times 6$ in (*a*), with each cube replaced with a $2 \times 2 \times 2$, $2 \times 2 \times 3$, $2 \times 3 \times 3$ or $3 \times 3 \times 3$ rectangular prismatic assembly with an associated MRP. For instance, the bottom left cube is to be replaced with a $2 \times 2 \times 3$ rectangular prismatic assembly with an MRP as shown in figure 2*c*. (Online version in colour.)

using MRPs for different sizes. The total number of links of such a rigidifying link pattern for $L \times M \times N$ is

$$\begin{aligned} &a_l a_m a_n \delta_{3D}(2) + b_l b_m b_n \delta_{3D}(3) + (a_l a_m b_n + a_l a_n b_m + a_m a_n b_l)\delta_{3D}(2,2,3) \\ &\quad + (a_l b_m b_n + a_m b_l b_n + a_n b_l b_m)\delta_{3D}(2,3,3) + \delta_{3D}(a_l + b_l) \\ &= 14 a_l a_m a_n + 52 b_l b_m b_n + 22(a_l a_m b_n + a_l a_n b_m + a_m a_n b_l) \\ &\quad + 34(a_l b_m b_n + a_m b_l b_n + a_n b_l b_m) + 2(a_l + b_l)(a_m + b_m)(a_n + b_n) - 2 \\ &= 2(2a_l + 3b_l)(2a_m + 3b_m)(2a_n + 3b_n) - 2 \\ &= 2LMN - 2. \end{aligned} \tag{2.13}$$

This implies that MRPs exist for $L \times M \times N$ and we have $\delta_{3D}(L, M, N) = 2LMN - 2$. ■

We remark that the technique in the proof above can be used recursively for constructing more MRPs. For instance, as $2 + 0 = 1 + 1 = 0 + 2 = 2$, by considering $(a_l, b_l, a_m, b_m, a_n, b_n) = (2, 0, 1, 1, 0, 2)$, we can construct an MRP for $4 \times 5 \times 6$ (figure 3*a*). Then, for any $a_l, b_l, a_m, b_m, a_n, b_n \geq 0$ with $a_l + b_l = 4, a_m + b_m = 5, a_n + b_n = 6$, we can use the same technique to construct an MRP for a $(2a_l + 3b_l) \times (2a_m + 3b_m) \times (2a_n + 3b_n)$ prismatic assembly. For instance, since $1 + 3 = 4$, $3 + 2 = 5$ and $5 + 1 = 6$, we can extend the construction in theorem 2.2 and create an MRP for a $(2 \times 1 + 3 \times 3) \times (2 \times 3 + 3 \times 2) \times (2 \times 5 + 3 \times 1) = 11 \times 12 \times 13$ rectangular prismatic assembly hierarchically (figure 3*b*). This shows the flexibility of our hierarchical construction framework for generating MRPs, which can be further used for creating rectangular prismatic assemblies with prescribed rigidity and connectivity.

As we can see in the proofs of theorem 2.1 and theorem 2.2, the two major components in the hierarchical construction of MRPs are: (i) the computation of the rigidity matrix for explicitly constructing small MRPs as the building blocks, and (ii) the integer partitioning of L, M, N in the form of $2m + 3n$ for recursively simplifying the problem. This combination of discrete mechanics and number theory provides a simple and useful framework for the design of prismatic assemblies.

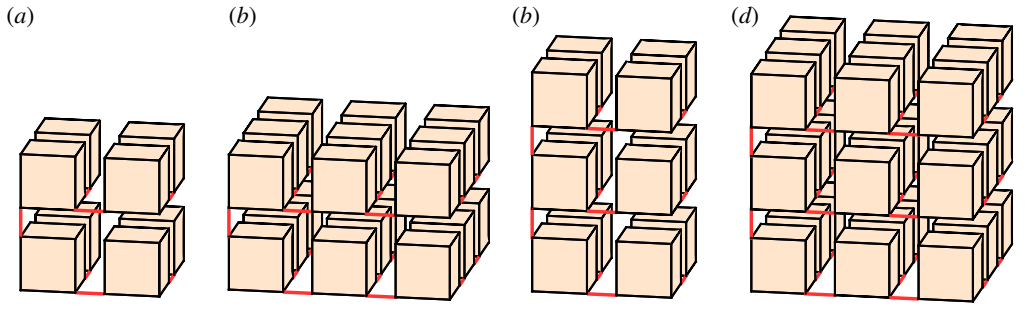

Figure 4. Examples of minimum connecting link patterns (MCPs) for rectangular prismatic assemblies. (*a*) An MCP for a $2 \times 2 \times 2$ rectangular prismatic assembly, with $2 \times 2 \times 2 - 1 = 7$ links. (*b*) An MCP for a $2 \times 3 \times 3$ rectangular prismatic assembly, with $2 \times 3 \times 3 - 1 = 17$ links. (*c*) An MCP for a $2 \times 2 \times 3$ rectangular prismatic assembly, with $2 \times 2 \times 3 - 1 = 11$ links. (*d*) An MCP for a $3 \times 3 \times 3$ rectangular prismatic assembly, with $3 \times 3 \times 3 - 1 = 26$ links. (Online version in colour.)

We note that in the two-dimensional case presented in [20], proving that the theoretical lower bound of the links for rigidification can be achieved requires multiple steps for handling different problem sizes (even number, odd primes, odd prime powers etc.). By contrast, as shown in the proof of theorem 2.1, the optimal lower bound for the three-dimensional case considered in this work can be achieved more directly without involving the complicated cases. Also, the two-dimensional approach presented in [20] focuses on the problem with $L \times L$ tiles. In the present work, in addition to solving the $L \times L \times L$ problem (theorem 2.1), we have shown how the hierarchical construction can be extended more broadly for tackling the $L \times M \times N$ problem with distinct L, M, N (theorem 2.2).

(b) Minimum connecting link patterns

Next, we consider the *minimum connecting link patterns* (MCPs), i.e. link patterns with the minimum number of links that can connect all cubes in a prismatic assembly. Denote $\gamma_{3D}(L, M, N)$ as the minimum number of links needed for connecting an $L \times M \times N$ prismatic assembly. Since NCC $= LMN$ when there is no link, and each link reduces the NCC by at most one, the minimum number of links is $\gamma_{3D}(L, M, N) = LMN - 1$. To construct MCPs, one may make use of the hierarchical construction with the building blocks being four MCPs for $2 \times 2 \times 2$, $2 \times 2 \times 3$, $2 \times 3 \times 3$ and $3 \times 3 \times 3$, which can be easily constructed (figure 4). For instance, we can obtain an MCP for a $5 \times 5 \times 5$ rectangular prismatic assembly using the decomposition shown in figure 2*e*, with each block connected by an MCP for $2 \times 2 \times 2$, $2 \times 2 \times 3$, $2 \times 3 \times 3$ and $3 \times 3 \times 3$, and all eight blocks connected by an MCP for $2 \times 2 \times 2$. Interestingly, $\delta_{3D}(L)$ and $\gamma_{3D}(L)$ are related by a simple formula

$$\delta_{3D}(L) = 2L^3 - 2 = 2(L^3 - 1) = 2\gamma_{3D}(L). \tag{2.14}$$

In other words, the minimum number of links needed for rigidifying any $L \times L \times L$ prismatic assembly is exactly twice that for connecting it.

(c) Simultaneous control of rigidity and connectivity using prescribed links

Denote the DoF in a prismatic assembly by d and the NCC by c. Using MRPs and MCPs, we can easily control the rigidity and connectivity of prismatic assembly and achieve different values of d and c simultaneously.

For any $L \times M \times N$ prismatic assembly with an MRP, there will be exactly six global modes (three translational and three rotational) without any overlaps and hence we have $d = 6$ and $c = 1$. Further adding links to it will not change either n or c. As links are removed, the dimension of

the nullspace of the rigidity matrix increases. More specifically, removing any k links from it will lead to an increase in d, making $d = 6 + 3k$. c will remain unchanged until $\delta_{3D}(L, M, N) - k$ reaches a certain threshold. We may also obtain a prismatic assembly with $d = 6pqr$ and $c = pqr$, where $p|L$, $q|M$ and $r|N$. This is achieved by reversing the process of the hierarchical construction and removing links at the coarsest level from an MRP.

For any $L \times M \times N$ prismatic assembly with an MCP, it is clear that $c = 1$ and $d = 6LMN - 3\gamma_{3D}(L, M, N) = 3LMN + 3$. Removing any k links from it will lead to an increase in c by k and an increase in d by $3k$, making $c = k + 1$ and $d = 3LMN + 3k + 3$. We remark that the maximum internal DoF of an $L \times M \times N$ prismatic assembly is $3LMN - 3$, which is achieved if the link pattern is an MCP. More specifically, the internal DoF is the total DoF less the six global DoF (three translational and three rotational) of each connected component in the assembly. As all cubes are connected by an MCP, there are only six global translational and rotational DoF in the entire system, and all the remaining DoF are internal DoF. Therefore, the internal DoF is $3LMN + 3 - 6 = 3LMN - 3$.

We remark that in our approach, the rigidity matrix computation yields infinitesimal floppy modes, and in general there are some floppy modes that violate the steric constraints that make it physically impossible once we go beyond the infinitesimal regime. The modes that do not violate the steric constraints indicate how the structure can be deployed rigidly, while those that do involve overlapping of assembly units provide us with information about the nature of the energetic cost of deforming the solids. For example, for each mode that involves overlapping, one can calculate the total energy cost associated with deforming the assembly and that with rotating around hinges, hence identifying the hierarchical energy/frequency spectrum of the whole assembly. Therefore, our approach can help in the design of structural assemblies of both rigid and soft objects.

3. Stochastic control of rectangular prismatic assemblies

Having explored the deterministic control of rigidity and connectivity in a prismatic assembly, we now explore controlling these quantities by adding or removing links randomly, a process that we will see leads to percolation transitions in rigidity and connectivity.

(a) Counting the total number of links

We calculate the total number of possible links in an $L \times L \times L$ rectangular prismatic assembly. First, it is easy to see that in the two-dimensional case of $L \times L$ quads, there are $2L(L-1)$ links along the x-direction and $2L(L-1)$ links along the y-direction. Therefore, the number of possible vertical or horizontal links in the three-dimensional case (i.e. the links which are parallel to some of the edges of the cubes) is given by

$$\begin{aligned} &2L(L-1) \times 2 \times L \text{ (along the } x\text{-direction)} + 2L(L-1) \times 2 \times L \text{ (along the } y\text{-direction)} \\ &\quad + 2L(L-1) \times 2 \times L \text{ (along the } z\text{-direction)} \\ &= 12L^2(L-1). \end{aligned} \tag{3.1}$$

As for the number of possible cross links, note that each space surrounded by eight cubes (like the centre of figure 1*b*) consists of 16 cross links, where 12 of them connect every pair of neighbouring cubes that share an edge, and 4 of them connect every pair of diagonally opposite cubes. More specifically, let v be the common vertex of the corners of eight neighbouring cubes, and denote the eight corners as $v_{-,-,-}$, $v_{-,-,+}$, $v_{-,+,-}$, $v_{-,+,+}$, $v_{+,-,-}$, $v_{+,-,+}$, $v_{+,+,-}$, $v_{+,+,+}$ based on the position of the centre of the cubes relative to v. Note that the vertical and horizontal links (such as $(v_{-,-,-}, v_{-,-,+})$ and $(v_{-,-,-}, v_{+,-,-})$) have already been counted earlier in §3a, and so they are not included in the counting of cross links. The 16 possible cross links include the 12 links that connect vertices with exactly two opposite signs, i.e. $(v_{\pm,-,-}, v_{\pm,+,+})$, $(v_{\pm,+,-}, v_{\pm,-,+})$, $(v_{-,\pm,-}, v_{+,\pm,+})$, $(v_{+,\pm,-}, v_{-,\pm,+})$, $(v_{-,-,\pm}, v_{+,+,\pm})$, $(v_{-,+,\pm}, v_{+,-,\pm})$, and the 4 links that connect

vertices with exactly three opposite signs, i.e. $(v_{-,-,-}, v_{+,+,+})$, $(v_{-,-,+}, v_{+,+,-})$, $(v_{-,+,-}, v_{+,-,+})$, $(v_{-,+,+}, v_{+,-,-})$. In an $L \times L \times L$ system, there are $(L-1) \times (L-1) \times (L-1)$ such spaces. Also, on each of the six sides of the rectangular prismatic assembly, there are $2(L-1)^2$ cross links. Therefore, the total number of cross links is

$$16(L-1)^3 + 6 \times 2 \times (L-1)^2 = 4(4L-1)(L-1)^2. \tag{3.2}$$

Hence, the total number of links n_{links} in an $L \times L \times L$ rectangular prismatic assembly is

$$n_{\text{links}} = 12L^2(L-1) + 4(4L-1)(L-1)^2 = 4(L-1)(7L^2 - 5L + 1). \tag{3.3}$$

(b) Simulation set-up

Denote $\rho \in [0,1]$ as the link density, i.e. the ratio of links randomly selected among all n_{links} possible links in the prismatic assembly. We sample random links with different ρ and study the DoF, NCC, and the size of the largest connected component T of the resulting prismatic assembly as a function of the link density. The total DoF is calculated based on equation (2.4), the NCC is calculated using a breadth-first search (BFS) algorithm in the prismatic assembly network and T is calculated after the BFS algorithm finds all connected components in the network. The internal rotational DoF is calculated as

$$d_{\text{int}} = d_{\text{tot}} - 6 \times \text{NCC}. \tag{3.4}$$

For each data point, 100 random link patterns with the same link density are generated, and the average values of the quantities above are presented in the figures. The SuiteSparse package (v. 5.7.1) is used for the rigidity matrix calculation (see [22] for the algorithmic details and implementation), and the experiments are performed on a computational cluster with up to 100 parallel threads.

(c) Simulation results

Figure 5 shows the simulation results using a $20 \times 20 \times 20$ prismatic assembly, which consists of 64 000 nodes (192 000 coordinates). We observe that the total DoF decreases rapidly as ρ increases, while the internal rotational DoF first increases and then decreases sharply (figure 5*a*). By increasing both the sampling frequency in between $\rho = 0$ and $\rho = 0.06$ and the number of repeats, we find that the peak of the internal DoF is at 0.036 (figure 5*a*, inset).

In the deterministic case, the maximum internal DoF is achieved by MCPs at the link density

$$\frac{\gamma_{3D}(L)}{n_{\text{links}}} = \frac{L^3 - 1}{4(L-1)(7L^2 - 5L + 1)} \to \frac{1}{28} \approx 0.0357, \tag{3.5}$$

which is very close to the peak density in the stochastic case. This is because when there are very few links, each newly added link is highly unlikely to be redundant, and thus most links reduce the total DoF by 3 and the NCC by 1, and increase the internal DoF by 2, until the assembly reaches the maximally floppy state. We note that the density at which the number of internal DoF reaches a maximum is much smaller than that in the planar analogue $L^2 - 1/(4L(L-1)) \to 1/4 = 0.25$ [20] as there are many more possible links in the three-dimensional case. Similar to the two-dimensional case studied previously [20], there is an exponential decay of DoF from $\rho = 0.04$ to 0.14, with $\log_{10} \text{DoF} \sim -15.5\rho$. Furthermore, the rotational DoF is dominant among all the DoF, the ratio of which attains its maximum at $\rho \approx 0.15$ (figure 5*b*). Both the range of dominance and its peak density are smaller than those in the two-dimensional case, because the NCC decreases more quickly as a function of ρ in the three-dimensional case (figure 5*c*). More specifically, NCC decays exponentially from $\rho = 0.03$ to 0.15, with $\log_{10} \text{NCC} \sim -20.8\rho$ (figure 5*c*, inset). The above maximum number of rotational DoF can also be understood in terms of the percolation transition in connectivity; indeed the size of the largest of connected component T reaches 1/2 at a similar link density (figure 5*d*).

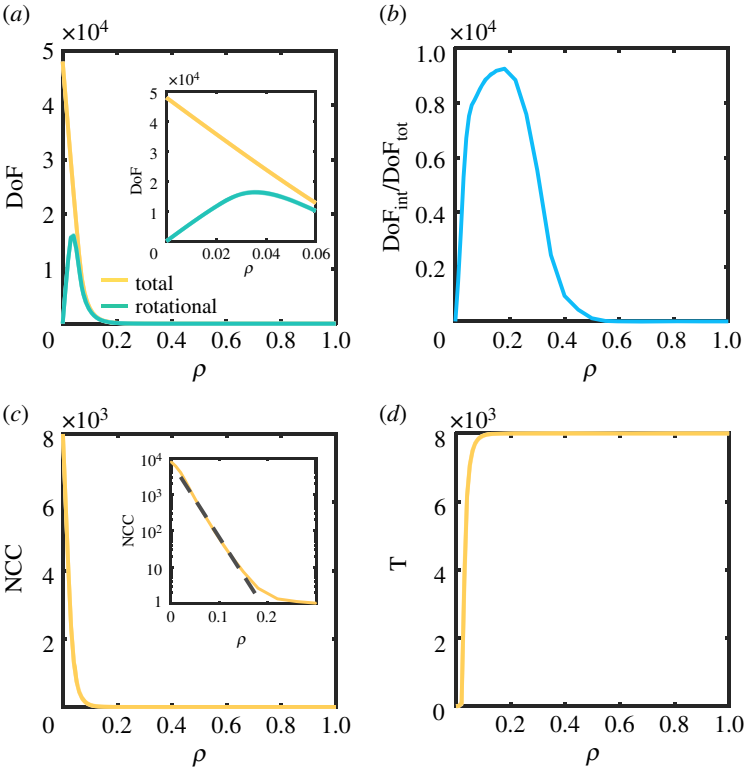

Figure 5. Stochastic control of prismatic assemblies. (*a*) The total DoF (yellow) and the internal rotational DoF (green) with varying link density ρ, with a zoom-in of the behaviour from $\rho = 0$ to 0.06 (inset). (*b*) The ratio between the rotational DoF and the total DoF. (*c*) The NCC with varying ρ in linear scale and in log scale (inset). (*d*) The size of the largest connected component (T) with varying ρ. The simulations are performed using a $20 \times 20 \times 20$ rectangular prismatic assembly. (Online version in colour.)

The stochastic control experiments were repeated for different system sizes ($L = 5, 10, 15, 20$). We can see the finite size effect in the normalized total and rotational DoF (figure 6*a*), the ratio between the rotational DoF and the total DoF (figure 6*b*), the NCC normalized by the system size L^3 (figure 6*c*) and the normalized size of the largest connected component T/L^3 (figure 6*d*). The finite size effect is clearer for $L = 5$, as the surface cubes take up $98/125 \approx 78\%$ of all the cubes. In addition, the derivative of DoF with respect to ρ is continuous (figure 6*a*, inset), suggesting that the rigidity percolation might be a second-order transition [10,24], consistent with most examples in two dimensions [4,25].

4. Triangular prismatic assemblies

Our study on the topological control of rectangular prismatic assemblies can be extended to other space-filling prisms, such as the triangular prisms.

(a) Minimum rigidifying link patterns

Note that each triangular prism consists of two triangular faces and three rectangular faces. Hence, there are in total nine edge length constraints and three diagonal length constraints for each prism. The DoF of an $L \times M \times N$ triangular prismatic assembly is then given by

$$d = 18LMN - \mathrm{rank}(A), \tag{4.1}$$

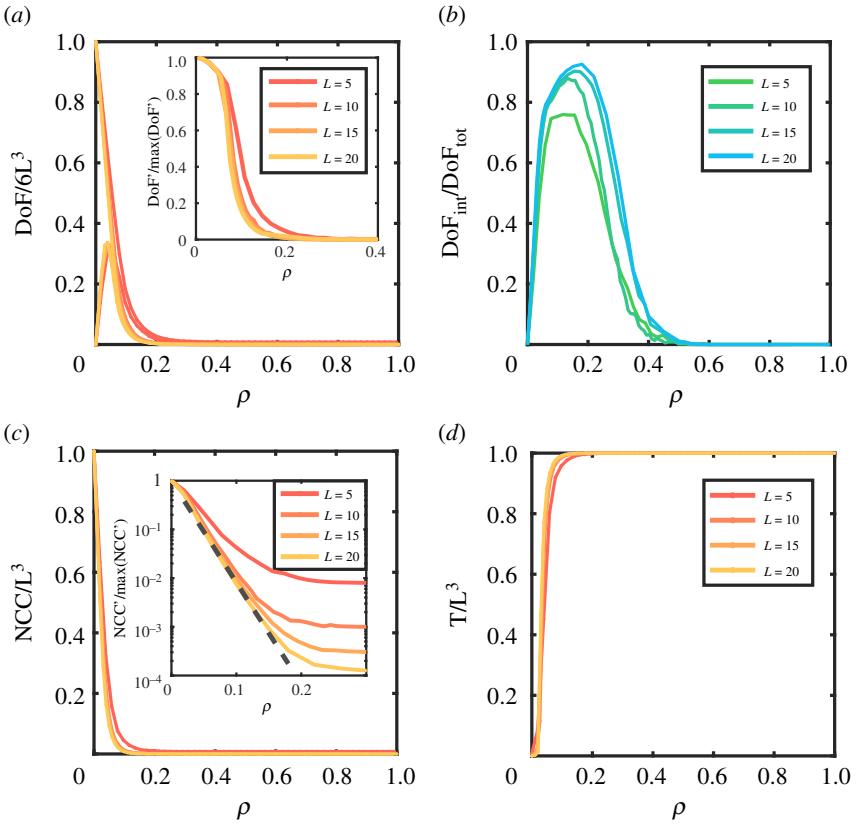

Figure 6. Stochastic control as a function of system size ($L = 5, 10, 15, 20$). (*a*) The normalized total and rotational DoF, with the derivative of the total DoF shown in the inset. (*b*) The ratio between the rotational DoF and total DoF. (*c*) The normalized NCC and the derivative of NCC with respect to ρ (inset). (*d*) The normalized size of the largest connected component T/L^3 as a function of the link density ρ. (Online version in colour.)

where A is a rigidity matrix with the dimension $(12LMN + 3n) \times 18LMN$. The factor 18 stems from the fact that each prism has six vertices, and each of them has three coordinates.

Let $\delta_\Delta(L, M, N)$ be the minimum number of links needed for rigidifying an $L \times M \times N$ triangular prismatic assembly. Using the same argument for the rectangular case, we have

$$\delta_\Delta(L, M, N) \geq 2LMN - 2. \tag{4.2}$$

Again, we call a link pattern with exactly $2LMN - 2$ links that can rigidify an $L \times M \times N$ triangular prismatic assembly an MRP. Using the hierarchical construction method, we can obtain the same result as in theorem 2.1 and theorem 2.2. The key idea is to explicitly construct MRPs for a set of small systems of size $2 \times 2 \times 2$, $2 \times 2 \times 3$, $2 \times 3 \times 2$, $3 \times 2 \times 2$, $2 \times 3 \times 3$, $3 \times 2 \times 3$, $3 \times 3 \times 2$ and $3 \times 3 \times 3$ as the building blocks (figure 7). By replacing the MRPs shown in figure 2 with these MRPs, we can prove that $\delta_\Delta(L) = 2L^3 - 2$ for all $L \geq 2$, and $\delta_\Delta(L, M, N) = 2LMN - 2$ for infinitely many L, M, N.

(b) Minimum connecting link patterns

Let $\gamma_\Delta(L, M, N)$ be the minimum number of links needed for connecting an $L \times M \times N$ triangular prismatic assembly. Analogous to the cubic case, it is easy to see that

$$\gamma_\Delta(L, M, N) = LMN - 1. \tag{4.3}$$

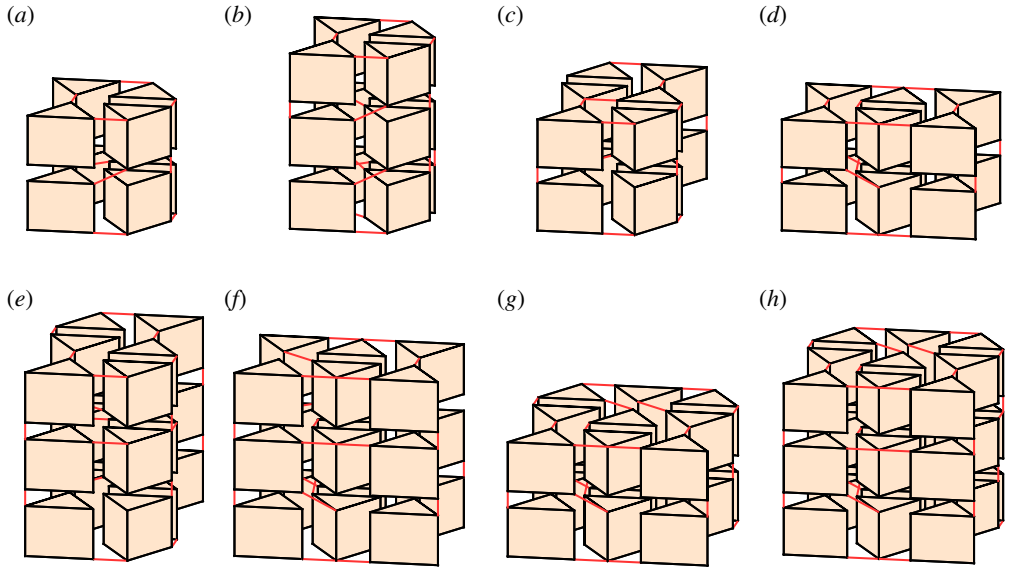

Figure 7. Minimum rigidifying link patterns (MRPs) for triangular prismatic assemblies. (*a*) An MRP for $2 \times 2 \times 2$, with $2 \times 2 \times 2 \times 2 - 2 = 14$ links. (*b*) An MRP for $2 \times 2 \times 3$, with $2 \times 2 \times 2 \times 3 - 2 = 22$ links. (*c*) An MRP for $2 \times 3 \times 2$, with $2 \times 2 \times 3 \times 2 - 2 = 22$ links. (*d*) An MRP for $3 \times 2 \times 2$, with $2 \times 3 \times 2 \times 2 - 2 = 22$ links. (*e*) An MRP for $2 \times 3 \times 3$, with $2 \times 2 \times 3 \times 3 - 2 = 34$ links. (*f*) An MRP for $3 \times 2 \times 3$, with $2 \times 3 \times 2 \times 3 - 2 = 34$ links. (*g*) An MRP for $3 \times 3 \times 2$, with $2 \times 3 \times 3 \times 2 - 2 = 34$ links. (*h*) An MRP for $3 \times 3 \times 3$, with $2 \times 3 \times 3 \times 3 - 2 = 52$ links. These eight patterns are the building blocks for hierarchically constructing MRPs for larger systems. (Online version in colour.)

To find an MCP for an $L \times M \times N$ triangular prismatic assembly, i.e. a link pattern with exactly $LMN - 1$ links that connect the entire system, we can simply use the construction approach for the rectangular case. The detail is omitted here.

Using the MRPs and MCPs, we can easily control the rigidity and connectivity of triangular prismatic assemblies.

5. Discussion

Our study of the topological control of prismatic assemblies provides novel strategies for achieving rigidity and connectivity via deterministic or stochastic cuts (corresponding to the creation and destruction of infinitesimal links), thereby yielding new insights into the design of structural assemblies. We note that the metric constraints associated with infinitesimal rigidity for solid cubes can be naturally extended to any rectangular solids, and hence our results for the deterministic and stochastic control hold for general rectangular prismatic assemblies. More specifically, in case the constituent prisms are not part of a regular grid, the link constraints are not affected. Thus although the scalar length constraints will be different, the rigidity matrix can be constructed in a similar manner. Our results can therefore be extended for controlling the rigidity and connectivity of other space-filling solids such as triangular prisms. A natural next step is to explore the control of rigidity and connectivity in three-dimensional assemblies formed by a tessellation of other polyhedra, including other space-filling polyhedra and their relatives such as the octet truss [26] or a combination of tetrahedra and octahedra [27].

In addition to the mode classification, we can also treat the links as springs with finite stiffness, thereby extending the infinitesimal rigidity theory to characterize the mechanical properties of the structural assembly [28]. The square roots of the eigenvalues of $A^T \Lambda A$, with Λ being the stiffness matrix, are the vibrational frequencies of such assemblies. In the absence of zero-frequency modes, the assembly becomes stiffer when new links are added. Therefore, by increasing the link density ρ, the peak of vibrational density of states shifts upwards. Additionally, the nature and

number of MRPs can assist the fine tuning of the vibrational density. For the same number of links, the distribution of links is more uniform in an MRP, i.e. the coefficient of variation in the frequency spectrum is small, compared with a random pattern where there are locally over-constrained and under-constrained areas, leading to a larger coefficient of variation in the spectrum. This suggests a means to further tune the spectrum by randomly moving the links in an MRP while keeping the total number of links the same, thus shifting the peak of the vibrational density of states towards higher frequencies, while creating a new peak at zero frequency.

We conclude with a discussion of how our results relate to considerations of marginally stable states, which have been important in the study of jamming in random networks [25,29–31]. The MRPs presented in this paper provide a new way of achieving marginal stability. In jamming networks and amorphous solids, systems achieve marginal stability near isostaticity [8]. Removal of contacts between particles generates DoF [30,31]. Similarly, removal of any link in an MRP increases the DoF. However, MRPs can be actively constructed using the hierarchical construction method, while the marginal stability in the systems above can be achieved only through pruning, either randomly or with certain protocols. This active construction is possible because of the highly repetitive geometry of the prismatic assemblies. In addition, the number of links in prismatic assemblies corresponding to the isostaticity state is $2dL^3 = 6L^3$ (d is the dimension), which is much larger than the number of links in an MRP ($\delta(L) \sim 2L^3$). Therefore, for the prismatic assemblies, the state of isostaticity and the constructed marginally stable state actually reside at two different link densities. With the recent works on tuning mechanical properties near the isostaticity state [11–15], another natural next step is to try tuning mechanical properties from the constructed marginally stable state (MRP) by introducing the spring network framework discussed above.

Data accessibility. The codes are available at the GitHub Repository https://github.com/garyptchoi/prismatic-assemblies. The link patterns for the deterministic control presented in figures 2, 4 and 7 can be generated and verified using the MATLAB codes provided. The patterns are also available in the form of MATLAB figure files for visualization. The simulation results for the stochastic control presented in figure 5 and figure 6 can be generated using the C++ codes provided.

Authors' contributions. G.P.T.C., S.C. and L.M. conceived and designed the research. G.P.T.C. and S.C. implemented and conducted the simulations in consultation with L.M. G.P.T.C., S.C. and L.M. analysed the results and wrote the manuscript. All authors gave final approval for publication and agree to be held accountable for the work performed therein.

Competing interests. We declare we have no competing interests.

Funding. This work was supported in part by the Harvard Quantitative Biology Initiative and the NSF-Simons Center for Mathematical and Statistical Analysis of Biology at Harvard, award no. 1764269 (to G.P.T.C. and L.M.), and NSF grants nos DMR 2011754, EFRI 1830901 and DMREF 1922321 (to L.M.).

References

1. Damasceno PF, Engel M, Glotzer SC. 2012 Predictive self-assembly of polyhedra into complex structures. *Science* **337**, 453–457. (doi:10.1126/science.1220869)
2. Fujita D, Ueda Y, Sato S, Mizuno N, Kumasaka T, Fujita M. 2016 Self-assembly of tetravalent Goldberg polyhedra from 144 small components. *Nature* **540**, 563–566. (doi:10.1038/nature20771)
3. Henzie J, Grünwald M, Widmer-Cooper A, Geissler PL, Yang P. 2012 Self-assembly of uniform polyhedral silver nanocrystals into densest packings and exotic superlattices. *Nat. Mater.* **11**, 131–137. (doi:10.1038/nmat3178)
4. Jacobs DJ, Thorpe MF. 1995 Generic rigidity percolation: the pebble game. *Phys. Rev. Lett.* **75**, 4051–4054. (doi:10.1103/PhysRevLett.75.4051)
5. Garboczi EJ, Snyder KA, Douglas JF, Thorpe MF. 1995 Geometrical percolation threshold of overlapping ellipsoids. *Phys. Rev. E* **52**, 819–828. (doi:10.1103/PhysRevE.52.819)
6. Chubynsky M, Briere M-A, Mousseau N. 2006 Self-organization with equilibration: a model for the intermediate phase in rigidity percolation. *Phy. Rev. E* **74**, 016116. (doi:10.1103/PhysRevE.74.016116)

7. Brière M-A, Chubynsky M, Mousseau N. 2007 Self-organized criticality in the intermediate phase of rigidity percolation. *Phy. Rev. E* **75**, 056108. (doi:10.1103/PhysRevE.75.056108)
8. van Hecke M. 2009 Jamming of soft particles: geometry, mechanics, scaling and isostaticity. *J. Phys. Condens. Matter* **22**, 033101. (doi:10.1088/0953-8984/22/3/033101)
9. Liu AJ, Nagel SR. 2010 The jamming transition and the marginally jammed solid. *Annu. Rev. Condens. Matter Phys.* **1**, 347–369. (doi:10.1146/annurev-conmatphys-070909-104045)
10. Chubynsky MV, Thorpe MF. 2007 Algorithms for three-dimensional rigidity analysis and a first-order percolation transition. *Phys. Rev. E* **76**, 041135. (doi:10.1103/PhysRevE.76.041135)
11. Goodrich CP, Liu AJ, Nagel SR. 2015 The principle of independent bond-level response: tuning by pruning to exploit disorder for global behavior. *Phys. Rev. Lett.* **114**, 225501. (doi:10.1103/PhysRevLett.114.225501)
12. Hexner D, Liu AJ, Nagel SR. 2018 Role of local response in manipulating the elastic properties of disordered solids by bond removal. *Soft Matter* **14**, 312–318. (doi:10.1039/C7SM01727H)
13. Reid DR, Pashine N, Wozniak JM, Jaeger HM, Liu AJ, Nagel SR, de Pablo JJ. 2018 Auxetic metamaterials from disordered networks. *Proc. Natl Acad. Sci. USA* **115**, E1384–E1390. (doi:10.1073/pnas.1717442115)
14. Liarte DB, Mao X, Stenull O, Lubensky T. 2019 Jamming as a multicritical point. *Phys. Rev. Lett.* **122**, 128006. (doi:10.1103/PhysRevLett.122.128006)
15. Liarte DB, Stenull O, Lubensky T. 2020 Multifunctional twisted kagome lattices: tuning by pruning mechanical metamaterials. *Phys. Rev. E* **101**, 063001. (doi:10.1103/PhysRevE.101.063001)
16. Dehn M. 1916 Über die starrheit konvexer polyeder. *Math. Ann.* **77**, 466–473. (doi:10.1007/BF01456962)
17. Philp D, Stoddart JF. 1996 Self-assembly in natural and unnatural systems. *Angew. Chem. Int. Ed. Engl.* **35**, 1154–1196. (doi:10.1002/anie.199611541)
18. Sun Q-F, Iwasa J, Ogawa D, Ishido Y, Sato S, Ozeki T, Sei Y, Yamaguchi K, Fujita M. 2010 Self-assembled $m_{24}l_{48}$ polyhedra and their sharp structural switch upon subtle ligand variation. *Science* **328**, 1144–1147. (doi:10.1126/science.1188605)
19. Zeravcic Z, Manoharan VN, Brenner MP. 2017 Colloquium: toward living matter with colloidal particles. *Rev. Mod. Phys.* **89**, 031001. (doi:10.1103/RevModPhys.89.031001)
20. Chen S, Choi GPT, Mahadevan L. 2020 Deterministic and stochastic control of kirigami topology. *Proc. Natl Acad. Sci. USA* **117**, 4511–4517. (doi:10.1073/pnas.1909164117)
21. Guest S. 2006 The stiffness of prestressed frameworks: a unifying approach. *Int. J. Solids Struct.* **43**, 842–854. (doi:10.1016/j.ijsolstr.2005.03.008)
22. Davis TA. 2011 Algorithm 915, SuiteSparseQR: multifrontal multithreaded rank-revealing sparse QR factorization. *ACM Trans. Math. Softw.* **38**, 1–22. (doi:10.1145/2049662.2049670)
23. Mao X, Lubensky TC. 2018 Maxwell lattices and topological mechanics. *Annu. Rev. Condens. Matter Phys.* **9**, 413–433. (doi:10.1146/annurev-conmatphys-033117-054235)
24. Huisman E, Lubensky TC. 2011 Internal stresses, normal modes, and nonaffinity in three-dimensional biopolymer networks. *Phys. Rev. Lett.* **106**, 088301. (doi:10.1103/PhysRevLett.106.088301)
25. Ellenbroek WG, Mao X. 2011 Rigidity percolation on the square lattice. *Europhys. Lett.* **96**, 54002. (doi:10.1209/0295-5075/96/54002)
26. Fuller RB. 1961 Octet truss. *U.S. Patent Serial No. 2, 986, 241*.
27. Conway JH, Jiao Y, Torquato S. 2011 New family of tilings of three-dimensional Euclidean space by tetrahedra and octahedra. *Proc. Natl Acad. Sci. USA* **108**, 11 009–11 012. (doi:10.1073/pnas.1105594108)
28. Thorpe M, Cai Y. 1989 Mechanical and vibrational properties of network structures. *J. Non-Cryst. Solids* **114**, 19–24. (doi:10.1016/0022-3093(89)90056-2)
29. Overvelde JT, Weaver JC, Hoberman C, Bertoldi K. 2017 Rational design of reconfigurable prismatic architected materials. *Nature* **541**, 347–352. (doi:10.1038/nature20824)
30. Sheinman M, Broedersz C, MacKintosh F. 2012 Actively stressed marginal networks. *Phys. Rev. Lett.* **109**, 238101. (doi:10.1103/PhysRevLett.109.238101)
31. Wyart M. 2012 Marginal stability constrains force and pair distributions at random close packing. *Phys. Rev. Lett.* **109**, 125502. (doi:10.1103/PhysRevLett.109.125502)